LANGMUIR Article
Cite This: Langmuir XXXX, XXX, XXX−XXX
pubs.acs.org/Langmuir

Surface and Interfacial Interactions in Dodecane/Brine Pickering Emulsions Stabilized by the Combination of Cellulose Nanocrystals and Emulsifiers

Sanjiv Parajuli,[†] Austin L. Dorris,[‡] Chadwick Middleton,[†] Andres Rodriguez,[†] Maren O' Haver,[†] Nathan I. Hammer,[‡] and Esteban Ureña-Benavides*[,†]

[†]Department of Chemical Engineering and [‡]Department of Chemistry and Biochemistry, University of Mississippi, University, Mississippi 38677, United States

Supporting Information

ABSTRACT: Interfacial properties of cellulose nanocrystals (CNC) and surfactants were studied in high ionic strength (I) brines and correlated to the stability of dodecane/brine Pickering emulsions. Bis-(2-hydroxyethyl) cocoalkylamine (CAA), dodecyltrimethylammonium bromide (DTAB), and octyl-β-D-glucopyranoside (OGP) were adsorbed onto CNC in American Petroleum Institute (API) brine (I = 1.9 M) and synthetic seawater (SSW), with I = 0.65 M. Raman spectroscopy indicated that hydroxyl groups on the CNC surface interact with all three surfactants in high ionic strength media. Ionic interactions still play a role at the very large ionic strengths studied herein. Despite all surfactants adsorbing onto CNC, only the surface tension of CAA solutions in both brines was increased by the addition of 0.5 wt % CNC. The effect was much more prominent in API than in SSW. Contact angle measurements indicated that CAA increased the wettability of CNC by both brines in dodecane; DTAB, on the other hand, decreased wettability. Emulsion stability studies revealed that ionic strength, wettability, adsorption energy, and oil content strongly affect emulsion stability, more so than surfactant adsorption. In API, CNC aggregates alone stabilized the emulsions better compared to samples with additional emulsifiers; the same was true in SSW for oil contents below 50% v/v. For oil contents above 50% v/v in SSW, CAA was either detrimental or failed to improve emulsion stability. On the other hand, DTAB increased the stability of dodecane in SSW emulsions. Emulsions stable for over 21 months were prepared with oil contents of 75% v/v. The adsorption of CAA onto CNC limits the migration of both CNC and CAA to the dodecane/brine interface, while DTAB adsorption has the opposite effect.

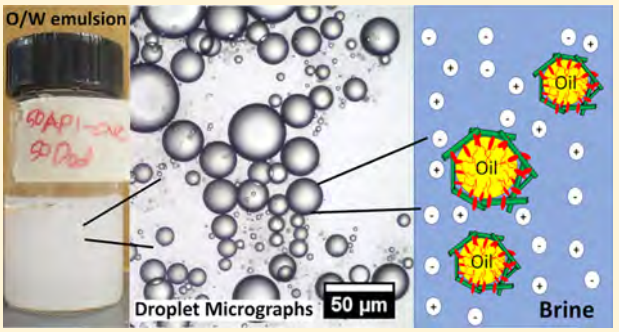

INTRODUCTION

Emulsions have applications both in daily life and in industries, and as the demand for stable formulations based on natural ingredients increases, there is a growing trend for using naturally occurring colloidal particles as emulsion stabilizers instead of surfactants.[1−3] Some of the common industrial applications of emulsions include food additives, oil-based creams, cosmetics, fertilizers, textile coatings, tertiary oil recovery, and oil spill cleanup.[4−8] Particle-stabilized (Pickering) emulsions have numerous advantages over traditional surfactant-stabilized emulsion including lower toxicity, low emulsifier content, and adjustable droplet size.[9−12] Emulsions prepared using only surfactants or nanoparticles have been extensively studied, but many commercial products of recent times have used a combination of surfactants and nanoparticles; therefore, it is important to understand how nanoparticles and surfactants interact and the mechanisms by which they stabilize emulsions. This understanding contributes to the efficient design and development of emulsion-based products.[13]

Charged nanoparticles such as silica, clay, gold, and cellulose nanocrystals (CNCs) are often used in conjunction with surfactants to stabilize emulsions.[14] Surfactants favor the formation of smaller emulsion droplets by lowering the interfacial tension between two phases; they also promote stability by preventing fluid drainage from droplets. Nanoparticles, on the other hand, do not significantly reduce the interfacial tension but, instead, migrate to and assemble at the liquid/liquid interface allowing stabilization of Pickering emulsions.[15] Pickering stabilization is a result of the nanoparticles forming a rigid structure around the droplet, which prevents droplet coalescence and Ostwald ripening.[16,17] The stabilization of emulsions by particles makes them more stable to coalescence as compared to surfactants because the energy associated with desorption of particles from the interface can be on the order of $10^3-10^4 k_B T$, whereas the energy required to

Received: April 25, 2019
Revised: August 14, 2019
Published: August 20, 2019

DOI: 10.1021/acs.langmuir.9b01218
Langmuir XXXX, XXX, XXX−XXX

desorb surfactants from the interface is two to three orders of magnitude smaller. This indicates that the adsorption of nanoparticles onto interfaces can essentially be considered irreversible.[18−20]

Few studies exist of Pickering emulsions in high-salinity brine. Worthen et al. reported improved stability of emulsified seawater/dodecane systems and CO_2 foams by a mixture of the zwitterionic surfactant caprylamidopropyl betaine and negatively charged silica nanoparticles as compared to a standalone surfactant or silica nanoparticles.[18,21] Binks et al. reported that mixtures of cationic surfactant CTAB and silica nanoparticles have synergistic effects on improving the stability of water/dodecane emulsions.[22] At a low concentration (0.1 wt %), the interaction between colloidal silica particles and nonionic surfactant Span 80 results in a lowered interfacial tension, thereby enhancing the stability of paraffin oil/water emulsions. Alternatively, at a higher surfactant concentration (1.8 wt %), emulsion stability was reduced.[23]

CNCs produced from bacterial cellulose was first used to stabilize hexane/water emulsions through ultrasonic mixing to produce monodisperse O/W emulsions that were stable for several months.[24] Hu and co-workers used 0.3 wt % cotton-derived CNCs alongside 0.2 wt % polymer solutions of hydroxyethyl cellulose, dextran, and methylcellulose to stabilize emulsions of water and dodecane.[25] Gestranius et al. also prepared O/W Pickering emulsions using CNF, tempo CNF, and CNCs in dodecane without using any surfactants. Emulsions prepared using CNF were stable to low shearing and an increase in temperature (up to 80 °C).[26] CNCs have been used to stabilize oil in water (O/W) emulsions in low-salinity aqueous phases. CNC dispersions in low-salinity brine (1000 ppm NaCl) were used to enhance crude oil mobility in sandstone cores for tertiary oil recovery at elevated temperatures and variable pH values. Viscosity measurements of the effluent revealed that most CNCs traverse the core.[7,27,28]

Despite the outburst in research involving CNC-stabilized emulsions, most studies have been conducted in low ionic strength (I) aqueous phases. Relatively little research has been done to explore the potential of CNCs as emulsion stabilizers in high ionic strength brines. Furthermore, the literature indicates that negatively charged particles have been used in combination with ionic and nonionic surfactants with varying degrees of success to stabilize emulsions in low ionic strength aqueous dispersions. This study attempts to elucidate the different outcomes obtained when different types of surfactants are added to Pickering emulsions. To achieve this goal, molecular interactions between CNCs and surfactants in high-salinity brines are studied via Raman spectroscopy, tensiometry, and adsorption measurements. The effect of those interactions on surface/interfacial properties are correlated to the stability of emulsions stabilized by CNCs and added emulsifiers in high-salinity aqueous solutions.

EXPERIMENTAL SECTION

Materials. Cellulose nanocrystals (11.5 wt %), prepared from *Pinus strobus* (Northern pine) wood pulp, made by the USDA Forest Products Laboratory and distributed by The University of Maine were used as received. Dodecane (99.9% reagent quality) was purchased from Sigma-Aldrich (St. Louis, MO) and used as received (unless otherwise specified). Dodecyltrimethylammonium bromide ≥90% (DTAB), Guar Gum, octyl-β-D-glucopyranoside (OGP), calcium chloride ($CaCl_2$), sodium chloride (NaCl), and synthetic seawater (SSW) were all purchased from Sigma-Aldrich and used as received. ETHOMEEN C/15, Bis (2-hydroxyethyl) cocoalkylamine (CAA), was kindly gifted by AkzoNobel (Houston, TX) and was used as received. The chemical structures of the emulsifiers used are depicted in the Supporting Information (SI), Figure S1. American Petroleum Institute (API) brine was prepared by adding 8 wt % NaCl and 2 wt % $CaCl_2$ in deionized (DI) water.

Characterization of CNCs. Atomic force microscopy (AFM) measurements were carried out using a Nanoscope IIIA multimode scanning probe microscope from Bruker (Billerica, MA). Topographic images obtained from AFM were processed using the Gwyddion software to measure the length and height of cellulose nanocrystals. The measurement of at least 100 rod-shaped individual crystals indicated that the average length of the particles was 128 ± 43 nm and the average height was 6.4 ± 1.8 nm, as shown in the SI, Figure S2. Conductometric titration of CNCs using methods explained elsewhere[29,30] indicated an average sulfur content of 0.045 ± 0.018 g-sulfur/g-cellulose on the surface of the CNCs used in this study (SI, Figure S3).

Adsorption Measurements. Adsorption of surfactants onto the CNC surface were measured using Shimadzu total organic carbon (TOC-L CSH E100) and total nitrogen (TNM-L) analyzer. Surfactant solutions in API (I = 1.9 M) brine and SSW (I = 0.65 M) were allowed to equilibrate with 1 wt % CNCs for at least 12 h, followed by centrifugation of the suspension to separate CNCs from the solution. The supernatant was carefully recovered and analyzed for the concentration of total organic carbon and total nitrogen. Equilibrium concentrations were plotted against the adsorbed concentration to generate adsorption isotherms of individual surfactants onto the CNC surface.

Raman Spectroscopy. A solid-state Horiba Labram HR Evolution Raman spectrometer (Horiba Instruments Inc, TX) using a 600 grooves/mm grating, 532 nm laser excitation, CCD camera detection, and a 100× micro-Raman objective was employed for the acquisition of Raman vibrational spectra. Vibrational Raman spectra of freeze-dried CNC dispersions in API brine and SSW were compared with the spectra of surfactant-adsorbed CNCs in both brines. Spectral signatures at a higher wavenumber corresponding to −OH stretching were analyzed for probable interactions between CNCs and surfactants. Prior to obtaining the spectra, surfactant solutions in brine and CNC dispersions were equilibrated for approximately 12 h. The dispersion was then centrifuged, and the pellet was recovered and allowed to sit in a hardened filter paper to remove excess water by capillary action. The pellet devoid of unadsorbed surfactants was then freeze-dried to remove excess water.

Surface Tension Measurements. The surface tension vs surfactant concentration plots in API brine and SSW (without CNCs in dispersion) were generated using a DuNuoy ring method after allowing the solution to equilibrate for 10 min using a force tensiometer, Sigma 701 (Nanoscience Instruments, Phoenix, Arizona). A surface tension vs surfactant concentration plot was also generated for each surfactant in the presence of 0.5 wt % CNC aggregates (or flocs) in brine, using axisymmetric pendant drop analysis with an Attension Theta Tensiometer (NanoScience Instruments, Phoenix, Arizona) after equilibrating for 60 min. Critical micelle concentration (CMC) of surfactants in brine was calculated in the presence and absence of CNC aggregates (or flocs). CMC calculated in the presence of CNCs is referred to as "apparent critical micelle concentration" (ACC).

Interfacial Tension Measurement. The interfacial tension between oil (dodecane) and an aggregated CNC dispersion in brine was measured using an optical tensiometer (NanoScience Instruments, Phoenix, AZ). Prior to the measurement of interfacial tension, *n*-dodecane was passed through an alumina column several times to remove impurities. The pendant drop method was used to perform axisymmetric drop shape analysis of a captive aqueous-phase drop in the presence of excess oil phase and after equilibrating with excess dodecane for 60 min, prior to taking measurements. Contours of the droplet's shape were fitted to the Young−Laplace equation to calculate the interfacial tension.[31]

DOI: 10.1021/acs.langmuir.9b01218
Langmuir XXXX, XXX, XXX−XXX

$$\Delta p = \rho gh - \gamma\left(\frac{1}{R_1} + \frac{1}{R_2}\right) \quad (1)$$

where Δp is the pressure difference across the interface, γ is the surface/interfacial tension, R_1 and R_2 are principal radii of curvature, and the term ρgh is the hydrostatic pressure.

Contact Angle Measurement. A thin film of CNCs was generated by adding a drop of 1 wt % CNC suspension in DI water onto freshly cleaved mica surface and drying overnight in a vacuum oven at 50 °C. The three-phase equilibrium static contact angle between the CNC film, surfactant solution (concentration near CMC in respective brine), and dodecane was measured using a sessile drop method in an Attension Theta optical tensiometer (NanoScience Instruments, Phoenix, AZ). Contact angles reported are the average of angles formed by both ends of the drop on the CNC film submerged in dodecane. At equilibrium, the phase contact angle is related to the interfacial tension by Young's equation.[21]

$$\cos\theta_{OW} = \frac{\gamma_{SO} - \gamma_{SW}}{\gamma_{OW}} \quad (2)$$

In the above equation, γ_{SO} is the interfacial tension between the solid surface and the oil phase, γ_{SW} is the interfacial tension between the solid surface and water, and γ_{OW} is the interfacial tension between oil and water.

Emulsion Preparation and Characterization. The aqueous phases of emulsions were prepared by adding surfactants to 200% brine; an equal volume part of 2 wt % CNC suspension was then added to the surfactant solution while mixing to prevent gelation. The final concentration of surfactants in the aqueous phase corresponds to their ACC in brine. The pH of the aqueous phase after the addition of surfactants was close to neutral, except for CAA, which was between pH 8 and 9. A total of 10 mL of *n*-dodecane in the aqueous phase was added to a 20 mL screw-capped vial with volume ratios ranging from 90 to 10% aqueous phase. The samples were then homogenized using a high-shear homogenizer (IKA Ultra-Turrax T-25 Basic, Atkinson, NH) at 10000 rpm for 1 min. Conductivity measurements using an Orion DuraProbe 4-Electrode Conductivity Cell having the Pt/Pt electrode were used to characterize emulsions as oil-in-water (O/W) or water-in-oil (W/O) type (SI Figure S4).

Emulsion Stability. Emulsion stability was measured in terms of droplet coalescence and creaming. Droplet coalescence was studied by monitoring the change in the emulsion droplet diameter over 24 h. The droplet diameter was measured by image analysis of optical micrographs created by an optical microscope (AmScope 500MD). A small aliquot of the emulsion was transferred from its vial to a microscopic slide by a spatula. A uniform layer of the emulsion was formed by placing a glass coverslip over the top of the emulsion drop, and droplets micrographs were analyzed using ImageJ to generate droplet size distribution. Emulsions' resistance to creaming was measured by monitoring the position of creaming front over a period of 24 h by analyzing pictures using ImageJ (U.S. NIH).

RESULTS AND DISCUSSION

Properties of CNCs and Surfactants in Brine. Colloidal stability of CNCs was diminished in the presence of electrolytes in the solution. Dynamic light scattering (DLS) measurements of 0.002 wt % CNC in DI water showed a hydrodynamic diameter of 164 nm, whereas in API and SSW, it was near 10 μm, indicating the aggregation of CNC in these brines. The addition of surfactants did not have a significant effect on the aggregation behavior of CNC in brines, with similar magnitude hydrodynamic diameters observed in the presence of surfactants. It should be pointed out that DLS measurements for aggregates above 1 μm only provide qualitative information. Visual examination of 1 wt % CNC suspensions in these brines showed that the particles do not precipitate within 26 h and remain suspended as aggregates (or flocs). The CMC and ACC of the surfactants were measured in the presence and absence of CNC aggregates (Table 1). The

Table 1. CMC for Emulsifiers in SSW and API Brine in the Presence and Absence of 0.5 wt % CNCs[a]

	CMC/ACC in API (g/L)		CMC/ACC in SSW (g/L)	
surfactant	w/CNCs	w/o CNCs	w/CNCs	w/o CNCs
OGP				
CAA	0.07 ± 0.06	0.01 ± 0.02	0.01 ± 0.03	0.01 ± 0.04
DTAB	0.16 ± 0.11	0.16 ± 0.03	0.67 ± 0.05	0.75 ± 0.05

[a]Errors represent standard errors

results indicate that, statistically, the CMC of surfactants did not change upon the addition of CNCs. The CMC of OGP is not reported, as no clear minimum was observed up to the concentration of 10 g/L.

Adsorption of Surfactants onto CNCs. The adsorption of surfactants onto the CNC surface was expressed in terms of the mass of the adsorbed surfactant per unit mass and unit area of CNCs. The area calculation assumes that flocs are sufficiently exfoliated to expose the area of individual CNCs; in reality, the exposed area must be smaller. The calculation of the adsorption per mass of CNC is unaffected by the aggregation state. Figure 1 indicates that in API brine, all

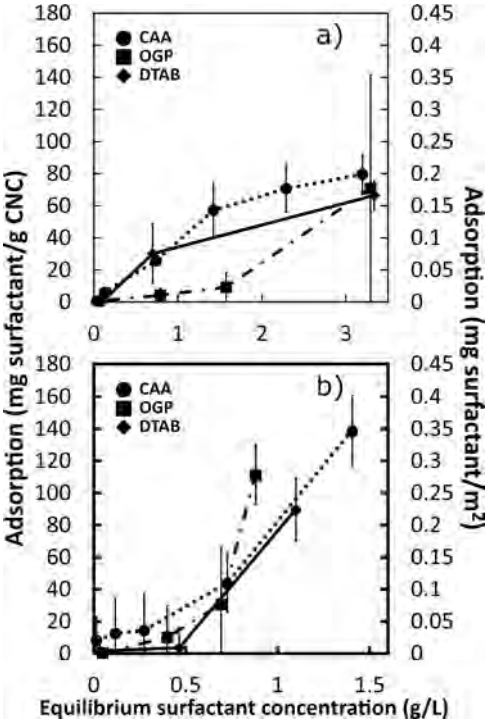

Figure 1. Isotherms for adsorption behavior of surfactants in API brine (a) and SSW (b). The lines are to guide the eye.

surfactants adsorb to a lesser extent compared to SSW. In API, all surfactants had a maximum adsorption ratio of nearly 0.22 g of the surfactant adsorbed per gram of the surfactant in the solution when the bulk concentration was 3 g/L. In SSW, however, the maximum adsorption ratios were 0.99 for CAA, 1.27 for DTAB, and 0.82 for OGP, when the equilibrium concentrations were 1.4, 0.88, and 1.10 g/L respectively. In the case of DTAB, higher adsorption in SSW could be due to the

DOI: 10.1021/acs.langmuir.9b01218
Langmuir XXXX, XXX, XXX−XXX

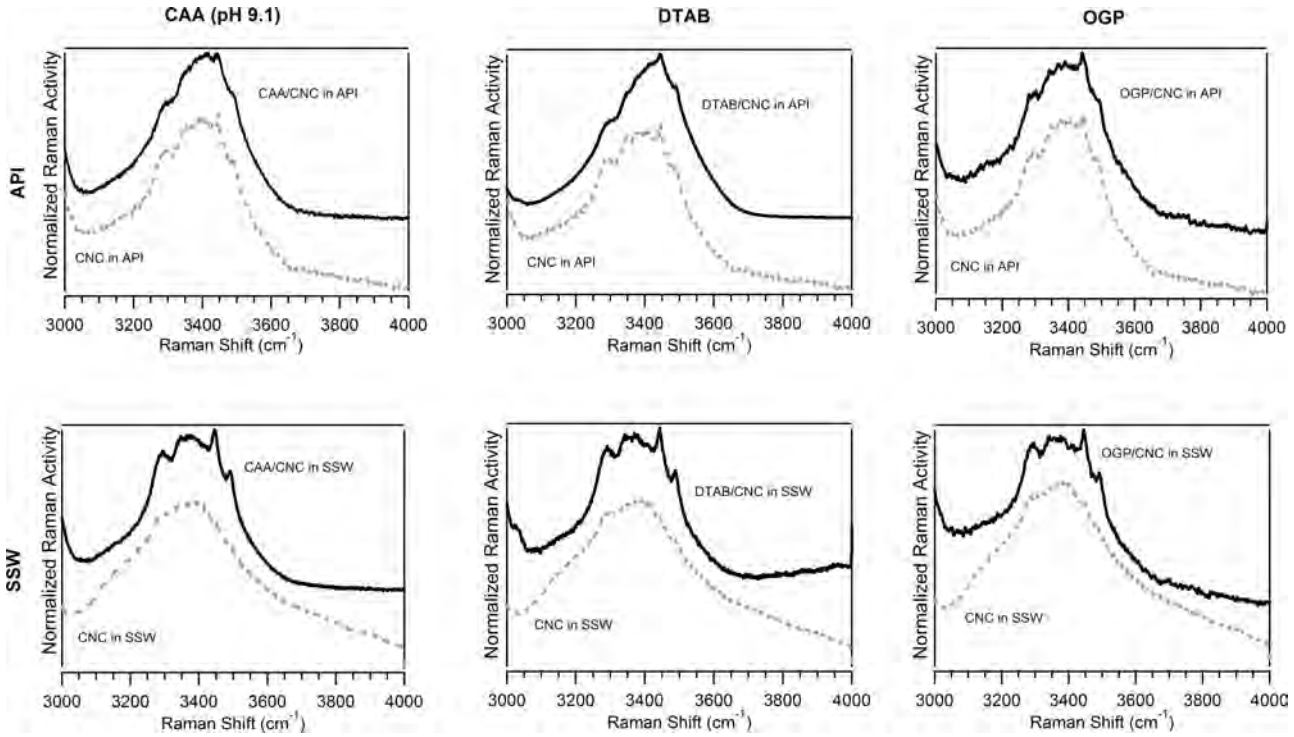

Figure 2. Raman spectra of CNCs in API brine (top panel) and SSW (bottom panel) in the presence and absence of CAA (left), DTAB (middle), and OGP (right).

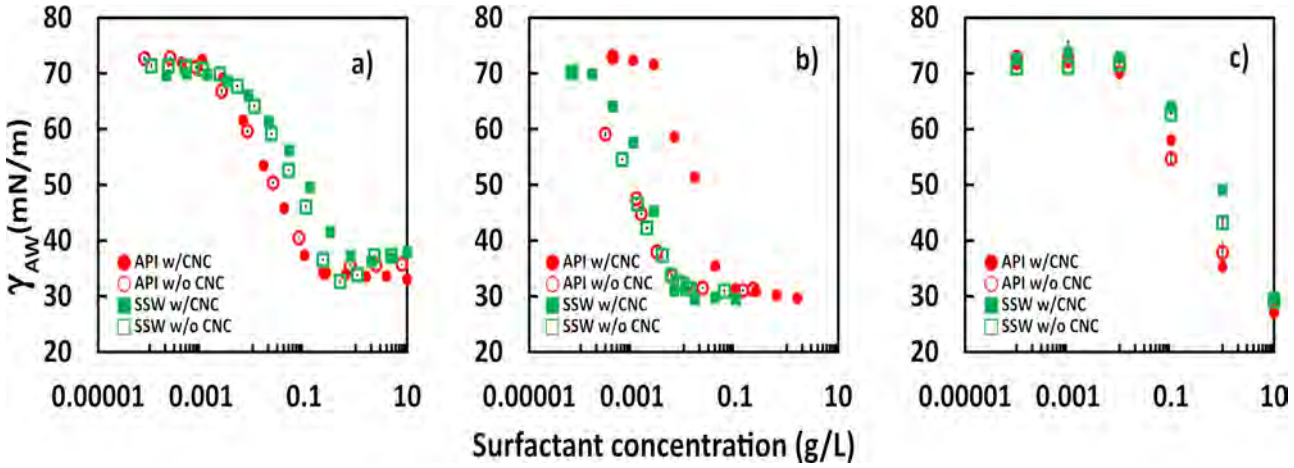

Figure 3. Air/API and air/SSW surface tensions (γ_{AW}) at various aqueous-phase concentrations of (a) DTAB, (b) CAA, and (c) OGP. The aqueous phase was either equilibrated with or without 0.5% w/w CNCs. The measured surface tension of pure API was 72.6 mN/m and that of SSW was 72.3 mN/m at room temperature. Errors indicate standard deviation.

lower ionic strength compared to API brine, which makes the former a better environment for ionic interactions between CNCs and the positively charged surfactant. Interestingly, the same trend is observed between CAA and OGP even though they bear a neutral headgroup at the conditions tested, suggesting that some other types of molecular interactions are also involved in the adsorption process.

Raman spectroscopy was used to elucidate other forms of intermolecular interactions between CNCs and the surfactants. Since CAA and OGP can both hydrogen bond to CNCs, special attention was paid to the −OH stretching signals (Figure 2). Addition of surfactants results in more structure in the −OH stretching region of cellulose nanocrystals in SSW; the effect was less evident in API. The different peak sharpness and definition suggest that −OH stretches are indeed sensitive probes to the CNC local environment. Such observations indicate the involvement of superficial hydroxyl groups of CNCs in the adsorption process, providing evidence for the presence of H-bonding between CNCs and surfactants in the complex mixtures.[32] However, the enhanced structure in the OH stretching region was also exhibited by DTAB, which cannot receive or donate H-bonds; this may indicate an ion−dipole type interaction between the charged DTAB and the −OH groups on CNCs. Interestingly, the Raman spectra observed after the addition of surfactant strongly resembles that of CNC nanoparticles prior to the introduction to either SSW or API. This is shown in the SI, Figure S5a−d. This strongly suggests that the surfactants are counteracting the

DOI: 10.1021/acs.langmuir.9b01218
Langmuir XXXX, XXX, XXX−XXX

effects of interactions by CNCs with species in the saltwater solutions.

Raman spectra of CAA adsorbed onto CNCs at different pH values in API brine were also measured. The structures in the −OH region were also affected by pH (SI Figure S6). At pH 10, when the amine group of CAA is negatively charged (SI, Figure S7), a sharp peak was observed with small shoulders on the sides. At a lower pH, where the amine group is protonated and positively charged, the −OH region was broader with less prominent peaks. The different peak patterns at variable pH values suggest that in API brine, along with ion−dipole and H-bonding interactions, short electrostatic interactions may also be important in the adsorption of CAA onto the CNC surface.

Surface Interactions and Adsorption. The adsorption behavior of each surfactant and CNCs was further studied through the dependence of surface tension (γ_{AW}) on the emulsifier concentration. Surface tension vs surfactant concentration plots for each surfactant were generated in the presence and absence of CNC aggregates (Figure 3). Upon addition of 0.5 wt % CNCs to a CAA-brine solution, the surface tension vs concentration plot shifts to the right; this effect is more prominent in API compared to SSW. Interestingly, despite adsorbing to the CNC surface, DTAB and OGP showed no significant curve shifting regardless of whether CNC aggregates were present in the dispersion or not. Such behavior suggests that in high ionic strength solutions, DTAB and OGP molecules preferentially migrate to the air−brine interface regardless of whether or not they adsorb onto CNCs. CAA, on the other hand, when adsorbed to the CNC surface does not migrate to the air/liquid interface and remain in the bulk. The observed trends, thus, suggest that the inability of a nanoparticle to increase the surface tension of a surfactant solution is not sufficient proof that the surfactant does not adsorb onto the nanoparticle.

Similar measurements carried out in DI water indicate that the adsorption of surfactants onto well-dispersed CNCs is expected to be primarily driven by electrostatic attractive forces between the emulsifier's charged headgroup and the negative CNC surface. In fact, the plot for DTAB does shift to a higher concentration in the presence of CNC when the experiment is done in DI water (SI, Figure S8), which is consistent with the existing literature.[33,34] Similarly, if the surfactant and nanoparticle charges are similar, the surfactant might not adsorb to the particle's surface but instead competes to occupy the fluid/fluid interface.[35] In brine, however, the electric double layer collapses resulting in closer proximity between CNCs, and between CNCs and the surfactants.[36,37] Thus, in concentrated electrolytes solutions, the interaction between CNCs and the emulsifiers is influenced by additional short-range intermolecular forces, which may include ion−dipole and H-bonding, in addition to electrostatic forces. This analysis is consistent with the vibrational Raman spectra, adsorption data, and surface tension measurements presented herein.

Interfacial Behavior of CNCs at the O/W Interface. The effect of CNC concentration on brine's surface tension (γ_{AW}) and dodecane−brine interfacial tension (γ_{OW}) was studied in API and SSW (Figure 4). CNCs do not alter the surface and interfacial tensions in DI water;[38] however, in high-salinity brine, CNCs lowered both, as shown in Figure 4. The surface activity exhibited by CNCs in brine occurs when they aggregate due to the collapse of the electrostatic double layer stabilizing individual nanocrystals. The CNC aggregates then migrate toward a surface where they can adsorb and assemble,

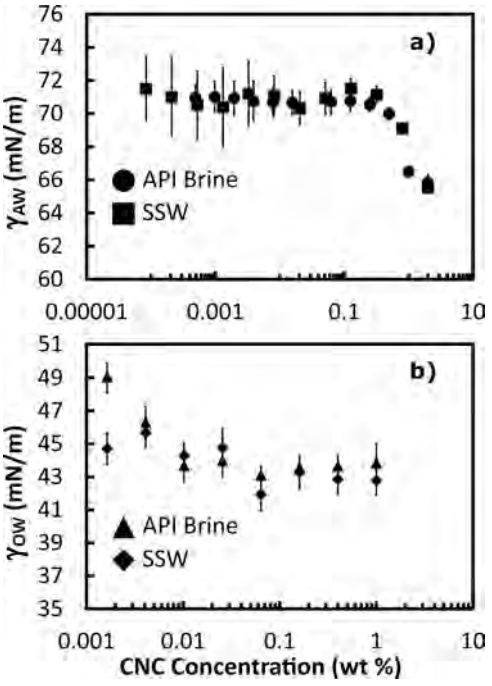

Figure 4. (a) Surface tension of CNC dispersions in brine and (b) interfacial tension of dodecane/brine as a function of CNC concentration. Errors indicate standard deviation.

lowering the surface and interfacial tensions. It has been discussed by Kalashnikova et al. that CNCs orient themselves at the oil−water interface with the hydrophobic (200) edge inside the oil phase, further justifying their surface activity.[39]

CNC Wettability and Adsorption Energy. Table 2 provides an overview of the contact angle (θ_{OW}) between the CNC film submerged in dodecane and surfactant solutions in brine, interfacial tension (γ_{OW}) between the two liquid phases, and the adsorption energy (ΔE_{rod}) of CNCs onto the oil−water interface. The reported adsorption energies are calculated for individual rod-shaped CNCs ignoring CNC−CNC interactions. The contact angle measurements were taken after allowing the drop of the surfactant solution to equilibrate with the CNC film for 100 s and are considered as equilibrium static contact angle. The CNC film showed swelling when the surfactant solution was left for more than 5 min on top of it. The authors consider the measurements before swelling to be a closer representation of the contact angle between CNCs, brine, and dodecane.

Table 2 indicates that the presence of CAA decreased the contact angle between brine and the CNC film; this was more prominent in SSW, which has a lower ionic strength. DTAB, on the other hand, increases the contact angle, thus decreasing wettability. These results signal that the addition of CAA to a CNC dispersion in brine increases the nanocrystal affinity toward the aqueous phase, whereas DTAB has the opposite effect.[40] Adsorption energies (ΔE_{rod}) were calculated for CNCs using eq 3, which was derived based on Pawel Pieranski's approach (SI Derivation 1). It assumes individual CNCs of cylindrical shape (radius r and length L), lying flat on the oil−water interface.[41]

$$\Delta E_{rod} = 2rL\gamma_{OW}(\theta_{OW}\cos\theta_{OW} - \sin\theta_{OW}) + \gamma_{OW}r^2\cos\theta_{OW}[2\theta_{OW} - \sin(2\theta_{OW})] \quad (3)$$

DOI: 10.1021/acs.langmuir.9b01218
Langmuir XXXX, XXX, XXX−XXX

Table 2. Three-Phase Contact Angle (θ_{OW}) between the CNC Film and Surfactant Solutions in Dodecane, and Interfacial Tension (γ_{OW}) between Liquid Phases and CNC Adsorption Energy (ΔE) onto the Oil/Brine Interface[a]

	API			SSW		
surfactants	θ_{OW} (deg)	γ_{OW} (mN/m)	ΔE_{rod} (kT)	θ_{OW} (deg)	γ_{OW} (mN/m)	ΔE_{rod} (kT)
none	28.2 ± 2.0	49.5 ± 0.8	−413	33.4 ± 3.0	46.7 ± 0.8	−643
DTAB	37.7 ± 1.3	12.8 ± 1.3	−253	42.0 ± 2.1	6.3 ± 1.6	−167
CAA	24.3 ± 4.2	14.9 ± 0.5	−80.2	23.8 ± 1.2	16.7 ± 1.1	−86.2

[a]Errors indicate standard error.

In eq 3, the first term arises from the lateral sides of the nanoparticles and the second term represents the contact area from the particle ends. As shown in Table 2, DTAB has more negative adsorption energy compared to CAA in both brines; however, the magnitude is even larger for CNC without surfactants. Thus, CNCs alone have the highest tendency to stay at the oil/water interface. When comparing between DTAB and CAA, the former leads to preferential adsorption to the interface. It must be pointed out that the CNCs in the aqueous phase are present as aggregates, and thus the magnitudes of ΔE in Table 2 are likely underestimated.

In addition to adsorption energy, the free energy of drop formation (ΔG_{drop}) given by eq 4 is also expected to have an effect on emulsion stability.[40,42]

$$\Delta G_{drop} = A_{OW}\gamma_{OW} + n_p(\Delta E_{ads} - T\Delta S_{ads}) \quad (4)$$

where A_{OW} is the interfacial the n_p is the number of particles. The effect of the entropy term (ΔS_{ads}) in the equation is expected to be relatively small for large particles like the ones used in this study. It is expected that systems with very negative ΔE_{ads} are conducive to small values of ΔG_{drop} and are more stable. Similarly, the low interfacial tensions of CAA and, to a greater extent, DTAB are also expected to lower ΔG_{drop} and improve emulsion stability.

Emulsion Stability. O/W emulsions were prepared using dodecane and 1 wt % CNC suspensions in a brine/surfactant solution. Negatively charged, individual CNCs were not able to form stable emulsions in DI water and phase separation occurred within 1 min of mixing; however, in high ionic strength brine, where CNCs are aggregated, it was possible to prepare stable emulsions (SI, Figure S9). Thus, for CNCs, decreasing colloidal stability by increasing the salt concentration enables the formation of Pickering emulsion.

The position of the creaming front was monitored for a period of 24 h by measuring the height of the aqueous phase eluted from the emulsion, as indicated in the SI, Figures S10 and S11. Emulsions in SSW were, in general, more stable to creaming compared to API. Emulsions prepared using CNCs only were most stable to creaming in most of the samples, the only exception being the emulsion prepared using DTAB + CNC in SSW with equal volume fractions of aqueous and organic phases (SI, Figure S11f). Emulsions containing CAA were the least-stable emulsions prepared; this is consistent with the very low contact angles, intermediate interfacial tension, and small adsorption energy observed for systems containing CAA in Table 2. According to Aveyard et al., colloidal particles with very large wettability are ineffective at stabilizing emulsions due to the particles remaining in the aqueous phase instead of adsorbing at the interface.[40] The combination of CNCs and CAA appears to be detrimental to emulsion stability.

Emulsions containing 25% v/v aqueous phase formed highly stable emulsions, as shown in Figure 5; remarkably, those

Figure 5. Pictures of representative stable emulsions taken after 6 months. Labels on vials indicate the aqueous to oil phase volume ratio and components in the aqueous phase. Emulsions enclosed inside the green box were still stable after 21 months.

inside the green box were stable to creaming for 21 months at the time of writing this article. On the contrary, the emulsions with 10% v/v aqueous phase separated quickly. At 25% v/v aqueous phase, the emulsions approach the phase inversion threshold, also evidenced by the low electric conductivity (Figure S4). However, since the CNCs/surfactant mixtures are highly hydrophilic, the emulsions do not invert phase, instead a high organic phase emulsion gel is formed.[40] At water contents lower than 25%, the highly hydrophilic particles cannot position themselves on the external side of the droplet and the emulsions cannot be stabilized.

Figure 5 and SI, Figure S11 indicate that as the oil fraction increases, the addition of DTAB becomes beneficial for emulsion stability in SSW but not in API brine. Interestingly, the adsorption energy of CNCs in DTAB is lower than for CNCs alone, which would indicate higher stability without the surfactant. However, in SSW, the interfacial tension γ_{OW} with DTAB is the lowest observed, which according to eq 4 should improve emulsion stability. Ultimately, the balance of these competing effects leads to a positive synergistic effect between DTAB and CNCs in SSW.

The stability of emulsions to coalescence was studied using optical micrographs of dodecane droplets over a period of 24 h (Figure 6). The coalescence results seem to follow a similar trend to creaming, with emulsions in SSW being more stable than those in API. Emulsions prepared using CNCs in API (Figure 6a) showed broadening and shifting of the droplet diameter peak, which was distinctly absent in the emulsions prepared in SSW, indicating that the latter are more stable to coalescence.

CNC Surface Coverage and Adsorption. The adsorption (Γ) of CNCs onto the dodecane−brine interface was

DOI: 10.1021/acs.langmuir.9b01218
Langmuir XXXX, XXX, XXX−XXX

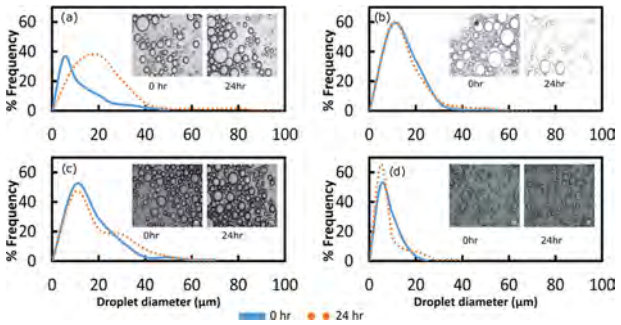

Figure 6. Droplet size distribution of representative emulsion samples with aqueous phases: (a) CNCs in API brine, (b) CNCs + DTAB in API brine, (c) CNCs in SSW, and (d) DTAB + CNCs in SSW. Each sample had 25% v/v aqueous phase and the emulsions were O/W type. Micrographs of dodecane droplets at t = 0 and 24 h are depicted as an image inset. The scale bar in the pictures represents 20 μm.

calculated for emulsions stabilized by CNC aggregates without surfactants according to eq 5.

$$\Gamma = \frac{m_p d_{avg}}{6V_{oil}} \tag{5}$$

The mass of CNCs at the interface, m_p, was measured from the concentration change of CNCs in the bulk aqueous phase eluted from the emulsions. The Sauter mean diameter, d_{avg}, was determined from the dodecane droplet size distribution. V_{oil} is the volume of the oil phase in the emulsion. Surface coverage (C) of emulsion droplets was estimated using eq 6.[43,44]

$$C = \frac{m_p d_{avg}}{6h_p \rho_p V_{oil}} \tag{6}$$

where h_p is the height of CNCs and ρ_p is the density of CNCs, which is equal to 1.64 g/cm^3. It should be noted that the derivation of eq 6 assumes that particles in the medium are dispersed without aggregation, and hence any values calculated are an overestimation of the actual coverage. This equation, however, is used to compare with the existing literature that uses the same method to quantify coverage.[24]

Table 3 shows the adsorption (Γ) and estimated surface coverage of CNCs at the brine/dodecane interface at different CNC concentrations in both API brine and SSW. The lowest surface coverage was 120 ± 6% for dodecane/SSW with 25% aqueous phase. Coverage increased with the decreasing oil content mainly due to the lower amount of the interface available. It was determined that all of the CNCs in the system adsorbed at the oil−water interface in all cases. Cherhal et al. estimated that a minimum of 84% cotton CNC coverage is required for the formation of Pickering emulsions stable for 1 month in a dilute 50 mM NaCl solution.[44] However, for the conditions tested here, surface coverage did not correlate to emulsion stability. In fact, the most stable emulsions were those with the lowest coverage, while the ones that creamed the most and broke fastest had 1800 ± 93% coverage. Assuming a maximum packing density of 0.9,[45] these adsorption amounts are equivalent to CNC crusts with minimum thicknesses of 12 nm for the most stable emulsion and 135 nm for the least-stable emulsion. Cherhal et al. studied the interfacial structure of CNCs in oil−water interfaces at different CNC concentrations and ionic strengths up to 50 mM. They found, through small-angle neutron scattering (SANS), that sulfated CNC in 50 mM solution formed interfacial layers with a thickness of 7 ± 0.5 nm. However, unsulfated CNCs, which aggregated in the aqueous medium, formed interfacial layers of 19 ± 0.5 nm thickness. Furthermore, SANS and wide-angle X-ray scattering results indicated that CNC interacted with oil interfaces through the hydrophobic (200) plane with exposed CH groups.[39,44]

The fact that the most stable emulsions prepared in this study had intermediate coverage indicate that multiple competing effects influence emulsion stability. As the thickness of the cellulose crust covering the oil droplet increases, van der Waals attraction forces between droplets also grow, given that they are proportional to the mass. In addition, a thicker CNC crust may increase the length and number of contact lines between oil, brine, and particles, leading to larger capillary forces. Both of these effects would reduce emulsion stability, as more CNCs are adsorbed onto the interface. On the other hand, the competing stabilizing effects of the CNC crust are expected to be steric repulsion between CNC aggregates on the surface and a large interfacial elasticity. The latter increases the drag force preventing droplets to approach each other by increasing the viscosity and elastic modulus of the interface.[46,47]

Inter-relation between CNCs and Surfactants. The data presented herein suggest that CAA adsorption onto the CNC surface is detrimental to the stability of dodecane emulsions in high ionic strength aqueous phases, whereas DTAB adsorption onto CNCs only improves emulsion stability at or above 50% v/v dodecane in SSW. The findings reported herein suggest that regardless of whether small molecule emulsifiers adsorb onto the CNCs or not, adsorption energies at the fluid/fluid interface and interfacial tension are deterministic properties for Pickering emulsion stabilization. This is consistent with confocal microscopy observations by Hu et al., which indicate that the HEC/CNC and MC/CNC particles adsorb at the fluid/fluid interface.[38]

Contact angle and surface tension measurements indicate that the adsorption of CAA onto CNCs increases their affinity toward brine, whereas DTAB adsorption has the opposite

Table 3. Adsorption and Surface Coverage of CNC Aggregates at Dodecane−Brine Interface Calculated Based on the Bulk Concentration of CNCs in the Aqueous Phase after Emulsification[a]

API			SSW		
aq. v/v % in emulsion	Γ (g/m^2)	coverage (%)	aq. v/v % in emulsion	Γ (g/m^2)	coverage (%)
90	0.58 ± 0.03	5600 ± 280	90	0.56 ± 0.02	5400 ± 300
75	0.20 ± 0.01	1800 ± 93	75	0.17 ± 0.01	1670 ± 90
50	0.060 ± 0.004	580 ± 30	50	0.059 ± 0.004	570 ± 30
25	0.018 ± 0.001	170 ± 10	25	0.012 ± 0.001	120 ± 6

[a]Errors indicate standard error.

DOI: 10.1021/acs.langmuir.9b01218
Langmuir XXXX, XXX, XXX−XXX

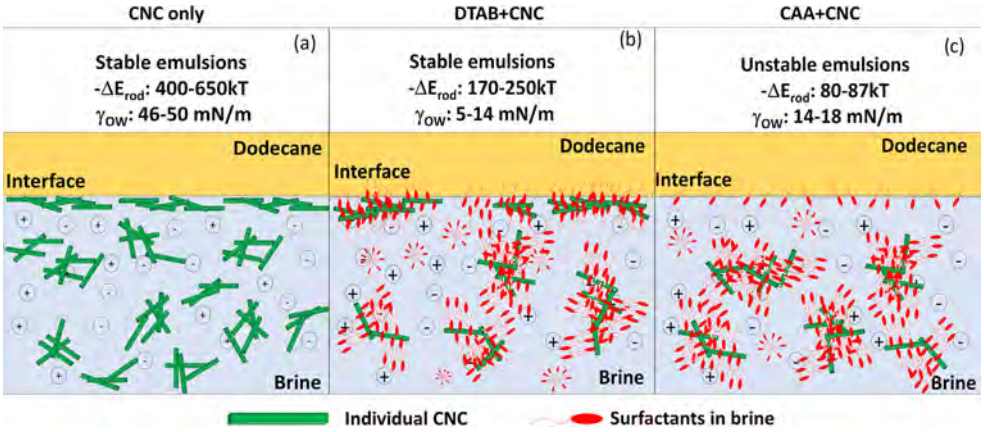

Figure 7. Schematics of (a) the assembly of CNC aggregates in brine and at the oil−water interface in the absence of surfactants, (b) assembly of CNCs and DTAB, where free DTAB molecules and CNCs-adsorbed DTAB migrate to the fluid−fluid interface, and (c) CAA assembly in the presence of CNCs where CAA- and CNCs-adsorbed CAA stay in the bulk aqueous phase; the surfactant forms a bilayer with the hydrophilic head protruding outward. The figure is not drawn to the scale.

effect. Such observation suggests that CAA, a twice ethoxylated surfactant with a large headgroup, forms a bilayer assembly on the CNC surface with the hydrophilic side protruding toward the bulk aqueous phase (Figure 7c). Such assembly would make the surfactant-coated CNCs less hydrophobic, though they remain aggregated. DTAB, which has a small headgroup in high-salinity solutions, adsorbs onto the CNC aggregates and diminishes their affinity toward the concentrated electrolyte solutions, thus aiding their migration to the dodecane−brine interface (Figure 7b). CNC aggregates in brine without surfactants readily adsorb onto the dodecane−brine interface and are efficient emulsion stabilizers (Figure 7a).

CONCLUSIONS

Surface interactions and interfacial behavior of CNC aggregates and several surfactants were studied in two high ionic strength solutions, synthetic seawater (SSW: I = 0.65 M) and American Petroleum Institute (API: I = 1.9 M) brine by means of Raman spectroscopy and interfacial properties. All surfactants studied adsorbed to the CNC surface in both SSW and API brine; however, adsorption was smaller in API. Raman spectra indicated that hydroxyl groups on the CNC surface were involved in the adsorption of small molecule surfactants, providing evidence that H-bonding drives the adsorption of the nonionic CAA and OGP onto CNCs. Hydroxyl groups were also involved in the adsorption of DTAB, which cannot H-bond, suggesting that other types of interaction, possibly ion−dipole, may drive their adsorption onto CNCs. The addition of 0.5 wt % CNCs to a CAA solution in API brine increased the surface tension by as much as 20 mN/m, whereas in SSW, the increment was just a few mN/m. Surprisingly, for DTAB and OGP, the surface tension vs. concentration curves in SSW and API nearly overlapped with and without CNCs, despite both surfactants adsorbing onto CNCs. This observation, along with contact angle measurements, suggests that DTAB and OGP migrate to fluid−fluid interfaces irrespective of whether they are adsorbed to CNCs or not. However, CAA, when adsorbed to CNCs, preferentially remains in the bulk aqueous phase.

Emulsion stability measurements with added surfactants show that the effect of surfactants is highly dependent on the dodecane content, interfacial tension, and CNC adsorption energy. CAA significantly decreases the magnitude of the CNC adsorption energy onto the oil/brine interface and consistently reduces emulsion stability. DTAB decreases the adsorption energy to a lesser extent but also lowers interfacial tension to 6.3 ± 1.6 mN/m in SSW and 12.8 ± 1.3 mN/m in API. Thus, DTAB improves emulsion stability of dodecane/SSW emulsions when the oil content approaches the phase inversion composition. However, in API brine, emulsions stabilized by CNC aggregates without surfactants were always the most stable. Emulsions stable for more than 21 months were prepared at 75% v/v dodecane content in SSW with added DTAB and in API brine without surfactants.

ASSOCIATED CONTENT

Supporting Information

The Supporting Information is available free of charge on the ACS Publications website at DOI: 10.1021/acs.langmuir.9b01218.

Chemical structures of emulsifiers, AFM image and size distribution of CNCs, sulfur content, identification of dispersed and continuous phases, Raman spectra of surfactants with and without CNCs, ζ-potential of surfactants, effect of CNCs on surface tension of surfactants in DI water, derivation of adsorption energy equation, emulsion stability in DI water and brine, creaming measurements of emulsions using different surfactants (PDF)

AUTHOR INFORMATION

Corresponding Author

*E-mail: eurenab@olemiss.edu.

ORCID

Sanjiv Parajuli: 0000-0001-6837-2749
Nathan I. Hammer: 0000-0002-6221-2709
Esteban Ureña-Benavides: 0000-0002-5525-488X

Notes

The authors declare no competing financial interest.

ACKNOWLEDGMENTS

The authors acknowledge the Donors of the American Chemical Society Petroleum Research Fund for support (or partial support) of this research. This research was also supported by the University of Mississippi Office of Research

DOI: 10.1021/acs.langmuir.9b01218
Langmuir XXXX, XXX, XXX−XXX

and Sponsored Programs. The authors would like to thank Dr. John O'Haver for his advice and insights. N.I.H. and A.L.D. acknowledge support from the National Science Foundation under grant numbers CHE-1532079 and OIA-1757220.

REFERENCES

(1) Pichot, R.; Spyropoulos, F.; Norton, I. T. Competitive adsorption of surfactants and hydrophilic silica particles at the oil–water interface: Interfacial tension and contact angle studies. *J. Colloid Interface Sci.* **2012**, *377*, 396–405.
(2) Madan, V.; Chanana, K.; Kataria, M. K.; Bilandi, A. Emulsion technology and recent trends in emulsion application. *Int. Res. J. Pharm. 5*, 533 542. DOI: 10.7897/2230-8407.0507108.
(3) French, D. J.; et al. The secret life of Pickering emulsions: particle exchange revealed using two colours of particle. *Sci. Rep.* **2016**, *6*, No. 31401.
(4) Frelichowska, J.; Bolzinger, M.-A.; Pelletier, J.; Valour, J.-P.; Chevalier, Y. Topical delivery of lipophilic drugs from o/w Pickering emulsions. *Int. J. Pharm.* **2009**, *371*, 56–63.
(5) Hunter, T. N.; Pugh, R. J.; Franks, G. V.; Jameson, G. J. The role of particles in stabilising foams and emulsions. *Adv. Colloid Interface Sci.* **2008**, *137*, 57–81.
(6) Gong, Y.; et al. A review of oil, dispersed oil and sediment interactions in the aquatic environment: Influence on the fate, transport and remediation of oil spills. *Mar. Pollut. Bull.* **2014**, *79*, 16–33.
(7) Molnes, S. N.; Mamonov, A.; Paso, K. G.; Strand, S.; Syverud, K. Investigation of a new application for cellulose nanocrystals: a study of the enhanced oil recovery potential by use of a green additive. *Cellulose* **2018**, *25*, 2289–2301.
(8) Molnes, S. N.; Torrijos, I. P.; Strand, S.; Paso, K. G.; Syverud, K. Sandstone injectivity and salt stability of cellulose nanocrystals (CNC) dispersions—Premises for use of CNC in enhanced oil recovery. *Ind. Crops Prod.* **2016**, *93*, 152–160.
(9) Du, W.; Guo, J.; Li, H.; Gao, Y. Heterogeneously Modified Cellulose Nanocrystals-Stabilized Pickering Emulsion: Preparation and Their Template Application for the Creation of PS Microspheres with Amino-Rich Surfaces. *ACS Sustainable Chem. Eng.* **2017**, *5*, 7514–7523.
(10) Chevalier, Y.; Bolzinger, M.-A. Emulsions stabilized with solid nanoparticles: Pickering emulsions. *Colloids Surf., A* **2013**, *439*, 23–34.
(11) Pickering, S. U. Emulsions. *J. Chem. Soc., Trans.* **1907**, *91*, 2001–2021.
(12) Ramsden, W. Separation of solids in the surface-layers of solutions and 'suspensions' (observations on surface-membranes, bubbles, emulsions, and mechanical coagulation).—Preliminary account. *Proc. R. Soc. London* **1904**, *72*, 156–164.
(13) Binks, B. P. Chapter 1: Emulsions — Recent Advances in Understanding. *Mod. Aspects Emulsion Sci.* **1998**, 1–55.
(14) Ma, H.; Luo, M.; Dai, L. L. Influences of surfactant and nanoparticle assembly on effective interfacial tensions. *Phys. Chem. Chem. Phys.* **2008**, *10*, 2207.
(15) Miao, C.; Tayebi, M.; Hamad, W. Y. Investigation of the formation mechanisms in high internal phase Pickering emulsions stabilized by cellulose nanocrystals. *Philos. Trans. R. Soc., A* **2018**, *376*, No. 20170039.
(16) Barnes, G.; Gentle, I. *Interfacial Science: An Introduction*; OUP Oxford, 2011.
(17) Eskandar, N. G.; Simovic, S.; Prestidge, C. A. Synergistic effect of silica nanoparticles and charged surfactants in the formation and stability of submicron oil-in-water emulsions. *Phys. Chem. Chem. Phys.* **2007**, *9*, 6426–6434.
(18) Worthen, A. J.; Bryant, S. L.; Huh, C.; Johnston, K. P. Carbon dioxide-in-water foams stabilized with nanoparticles and surfactant acting in synergy. *AIChE J.* **2013**, *59*, 3490–3501.
(19) Capron, I.; Rojas, O. J.; Bordes, R. Behavior of nanocelluloses at interfaces. *Curr. Opin. Colloid Interface Sci.* **2017**, *29*, 83–95.
(20) Akartuna, I.; Studart, A. R.; Tervoort, E.; Gonzenbach, U. T.; Gauckler, L. J. Stabilization of Oil-in-Water Emulsions by Colloidal Particles Modified with Short Amphiphiles. *Langmuir* **2008**, *24*, 7161–7168.
(21) Worthen, A. J.; et al. Synergistic Formation and Stabilization of Oil-in-Water Emulsions by a Weakly Interacting Mixture of Zwitterionic Surfactant and Silica Nanoparticles. *Langmuir* **2014**, *30*, 984–994.
(22) Binks, B. P.; Rodrigues, J. A.; Frith, W. J. Synergistic Interaction in Emulsions Stabilized by a Mixture of Silica Nanoparticles and Cationic Surfactant. *Langmuir* **2007**, *23*, 3626–3636.
(23) Nesterenko, A.; Drelich, A.; Lu, H.; Clausse, D.; Pezron, I. Influence of a mixed particle/surfactant emulsifier system on water-in-oil emulsion stability. *Colloids Surf., A* **2014**, *457*, 49–57.
(24) Kalashnikova, I.; Bizot, H.; Cathala, B.; Capron, I. New Pickering Emulsions Stabilized by Bacterial Cellulose Nanocrystals. *Langmuir* **2011**, *27*, 7471–7479.
(25) Hu, Z.; Patten, T.; Pelton, R.; Cranston, E. D. Synergistic Stabilization of Emulsions and Emulsion Gels with Water-Soluble Polymers and Cellulose Nanocrystals. *ACS Sustainable Chem. Eng.* **2015**, *3*, 1023–1031.
(26) Gestranius, M.; Stenius, P.; Kontturi, E.; Sjöblom, J.; Tammelin, T. Phase behaviour and droplet size of oil-in-water Pickering emulsions stabilised with plant-derived nanocellulosic materials. *Colloids Surf., A* **2017**, *519*, 60–70.
(27) Molnes, S. N.; Paso, K. G.; Strand, S.; Syverud, K. The effects of pH, time and temperature on the stability and viscosity of cellulose nanocrystal (CNC) dispersions: implications for use in enhanced oil recovery. *Cellulose* **2017**, *24*, 4479–4491.
(28) Monclin, J.-P.; Nelson, K.; Retsina, T. Drilling fluid additives and fracturing fluid additives containing cellulose nanofibers and/or nanocrystals. U.S. patent US20170240792A12015, pp 1 18.
(29) Abitbol, T.; Kloser, E.; Gray, D. G. Estimation of the surface sulfur content of cellulose nanocrystals prepared by sulfuric acid hydrolysis. *Cellulose* **2013**, *20*, 785–794.
(30) Dong, H.; et al. Cellulose nanocrystals as a reinforcing material for electrospun poly(methyl methacrylate) fibers: Formation, properties, and nanomechanical characterization. *Carbohydr. Polym.* **2012**, *87*, 2488–2495.
(31) Berry, J. D.; Neeson, M. J.; Dagastine, R. R.; Chan, D. Y. C.; Tabor, R. F. Measurement of surface and interfacial tension using pendant drop tensiometry. *J. Colloid Interface Sci.* **2015**, *454*, 226–237.
(32) Agarwal, U. P. 1064 nm FT-Raman spectroscopy for investigations of plant cell walls and other biomass materials. *Front. Plant Sci.* **2014**, *5*, 490.
(33) Kedzior, S. A.; Marway, H. S.; Cranston, E. D. Tailoring Cellulose Nanocrystal and Surfactant Behavior in Miniemulsion Polymerization. *Macromolecules* **2017**, *50*, 2645–2655.
(34) Dhar, N.; Au, D.; Berry, R. C.; Tam, K. C. Interactions of nanocrystalline cellulose with an oppositely charged surfactant in aqueous medium. *Colloids Surf., A* **2012**, *415*, 310–319.
(35) Binks, B. P.; Desforges, A.; Duff, D. G. Synergistic Stabilization of Emulsions by a Mixture of Surface-Active Nanoparticles and Surfactant. *Langmuir* **2007**, *23*, 1098–1106.
(36) Mcbride, M. B. A critique of diffuse double layer models applied to colloid and surface chemistry. *Clays Clay Miner.* **1997**, *45*, 598–608.
(37) Hiemenz, P. C.; Rajagopalan, R. *Principles of Colloids and Surface Chemistry*; Marcel Dekker Inc, 1997.
(38) Hu, Z.; Ballinger, S.; Pelton, R.; Cranston, E. D. Surfactant-enhanced cellulose nanocrystal Pickering emulsions. *J. Colloid Interface Sci.* **2015**, *439*, 139–148.
(39) Kalashnikova, I.; Bizot, H.; Cathala, B.; Capron, I. Modulation of Cellulose Nanocrystals Amphiphilic Properties to Stabilize Oil/Water Interface. *Biomacromolecules* **2012**, *13*, 267–275.
(40) Aveyard, R.; Binks, B. P.; Clint, J. H. Emulsions stabilised solely by colloidal particles. *Adv. Colloid Interface Sci.* **2003**, *100–102*, 503–546.

DOI: 10.1021/acs.langmuir.9b01218
Langmuir XXXX, XXX, XXX–XXX

(41) Pieranski, P. Two-Dimensional Interfacial Colloidal Crystals. *Phys. Rev. Lett.* **1980**, *45*, 569−572.
(42) Aveyard, R.; Clint, J. H.; Horozov, T. S. Aspects of the stabilisation of emulsions by solid particles: Effects of line tension and monolayer curvature energy. *Phys. Chem. Chem. Phys.* **2003**, *5*, 2398.
(43) Kalashnikova, I.; Bizot, H.; Bertoncini, P.; Cathala, B.; Capron, I. Cellulosic nanorods of various aspect ratios for oil in water Pickering emulsions. *Soft Matter* **2013**, *9*, 952−959.
(44) Cherhal, F.; Cousin, F.; Capron, I. Structural Description of the Interface of Pickering Emulsions Stabilized by Cellulose Nanocrystals. *Biomacromolecules* **2016**, *17*, 496−502.
(45) The packing density of 0.9 corresponds to hexagonally packed cylinders. In reality, the CNC shape is closer to elongated particles with octagonal cross-sections. This value is only an upper limit.
(46) Butt, H.-J.; Kappl, M. *Surface and Interfacial Forces*; Wiley-VCH, 2010.
(47) van den Berg, M. E. H.; et al. Modifying the Contact Angle of Anisotropic Cellulose Nanocrystals: Effect on Interfacial Rheology and Structure. *Langmuir* **2018**, *34*, 10932−10942.

DOI: 10.1021/acs.langmuir.9b01218
Langmuir XXXX, XXX, XXX−XXX